ЖУРНАЛ СТРУКТУРНОЙ ХИМИИ

*2017. Том 58, № 7* *Сентябрь – октябрь* *С. 1347 – 1357*

UDC 541.67:548.73:546.72

# THEORETICAL APPROACH TO THE MOLECULAR STRUCTURE, CHEMICAL REACTIVITY, MOLECULAR ORBITAL ANALYSIS, SPECTROSCOPIC PROPERTIES (IR, UV, NMR), AND NBO ANALYSIS OF DEFERIPRONE

**A. Valizadeh[1,2,3], R. Ghiasi[4]**

[1]*Department of Medical Nanotechnology, Faculty of Advanced Medical Sciences, Tabriz University of Medical Sciences, Tabriz, Iran*
[2]*Student Research Committee, Tabriz University of Medical Sciences, Tabriz, Iran*
[3]*Department of Medical Nanotechnology, School of Advanced Technologies in Medicine, Tehran University of Medical Sciences, Tehran, Iran*
[4]*Department of Chemistry, East Tehran Branch, Islamic Azad University, Tehran, Iran*
E-mail: rezaghiasi1353@yahoo.com

*Received December, 15, 2015* *Revised April, 11, 2016*

In this investigation, the structural, electronic properties, $^{13}C$ and $^{1}H$ NMR parameters and the first hyperpolarizability of deferiprone are computed in the gas phase and various solvents at the M062X/6-311++G(*d*,*p*) level of theory. The solvent effect on the structural parameters, frontier orbital energies, $^{13}C$ and $^{1}H$ NMR parameters is also explored based on a polarizable continuum model. These consequences specify that the polarity of solvents affects the structures and spectroscopic properties of deferiprone. $^{1}H$ and $^{13}C$ NMR chemical shifts are evaluated by employing the gauge-invariant atomic orbital method. NBO analysis is exploited to examine the hybridization of atoms, atomic charges, and their second order stabilization energy within the molecule.

DOI: 10.26902/JSC20170706

**K e y w o r d s:** deferiprone, frontier orbital analysis, $^{1}H$ and $^{13}C$ NMR calculations, NBO analysis.

## INTRODUCTION

Deferiprone (the IUPAC chemical name is 3-hydroxy-1,2-dimethylpyridin-4(1H)-one, trade name Ferriprox) belongs to the family of alpha-ketohydroxypyridines. Deferiprone is the only orally administered iron chelator drug approved for the clinical use in treatment of β-thalassemic patients [ 1 ]. These chelators have a high binding affinity to iron. Thus, deferiprone is able to remove iron from proteins that are transporting and storing iron in the body [ 2 ]. Within the transfused red cells iron accumulates inexorably and excess iron damages the liver, endocrine organs, and heart, which may be fatal for β-thalassemic patients by adolescence without concomitant chelation therapy [ 1d, 3 ]. Transfusion and iron chelation treatment have significantly improved survival and reduced morbidity in β-thalassemic patients during the last three decades [ 2a, 4 ].

This drug is also used to treat cancer, leukemia, renal insufficiency and other diseases [ 5 ]. In treatment of cancer by this drug it inhibited cellular iron uptake, increased transferrin receptor protein and mRNA levels, and decreased intracellular ferritin level [ 6 ]. The results show that by these mechanisms deferiprone inhibits HepG2 cell proliferation and blocks the cell cycle in the S phase [ 6 ].

Also, deferiprone is used to inhibit HIV-1 replication in a tissue culture by inhibiting the enzyme deoxyhypusine hydroxylase (DOHH) [ 7 ] required for maturation of eukaryotic translation initiation factor eIF5A implicated in HIV-1 replication [ 7b ]. Due to DOHH inhibition, eIF5A is not activated, and then it represses expression from the HIV-1 promoter at the level of transcription initiation [ 7b ]. Also, deferiprone can inhibit nuclear factor-κB activation and the subsequent replication of HIV-1 [ 8 ]. Furthermore, it can render iron-dependent ribonucleotide reductase inactive, thereby inhibiting the DNA synthesis and HIV replication, respectively [ 9 ].

The solvent effect plays an extensive and insightful role in numerous chemical characteristics, such as the properties of systems in the chemical equilibrium, rates and stereoselectivity of reactions, and spectra. Based on the traditional non-equilibrium solvation theory, various continuum solvation models, e.g. the polarizable continuum model (PCM) [ 10 ], have been developed. Biological processes occur in solvents; therefore, the understanding of solvent effects is essential for an exact classification of many chemical and biochemical systems.

In this paper, we illustrate the structure, vibrational spectrum, electronic properties, $^{13}C$ and $^{1}H$ NMR parameters, and electronic spectra of deferiprone at the M062X/6-311++G(*d*,*p*) level.

## COMPUTATIONAL METHOD

The Gaussian 09 suite of programs was applied to carry out all calculations [ 11 ]. The standard 6-311++G(*d*,*p*) basis set [ 12 ] and the hybrid functional of Truhlar and Zhao (M062X) [ 13 ] were used for the optimization of the molecule. To study the solvation effects, all structures were reoptimized in the solution by a self-consistent reaction field (SCRF) approach, in particular using the PCM [ 10 ].

A vibrational analysis was carried out after the optimization at each stationary point found. The result of this analysis confirms its identity as an energy minimum.

The population analysis has also been performed by the natural bond orbital method [ 14 ] using the NBO program [ 15 ] using the Gaussian 2009 program package at the M062X/6-311++G(*d*,*p*) level of theory.

The assignments of all the normal vibrational modes have been made based on the calculated potential energy distributions (PEDs). For the calculation of PEDs the vibrational problem was set up in terms of internal coordinates using the VEDA software [ 16 ].

NMR calculations were performed using the Gauge independent atomic orbital (GIAO) [ 17 ] method at the M062X/6-311++G(*d*,*p*) level of theory.

The electronic spectra of the studied molecule were calculated by TD-DFT [ 18 ] using the same hybrid functionals and the basis set as those used for the optimization. The 30 lowest excitation energies were calculated.

## RESULTS AND DISCUSSION

**Energy.** Fig. 1, *a* presents the molecular structure of the deferiprone molecule. The energies of the deferiprone molecule in the gas phase and different media are gathered in Table 1. $E_T$ and $E_{solv}$ are

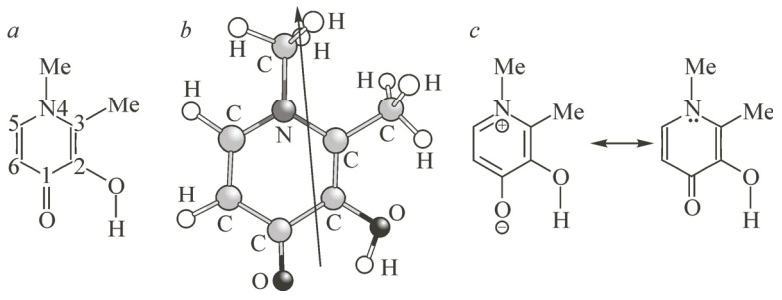


*Fig. 1.* Structure (*a*), direction of dipole moment (*b*), and resonance forms of the deferiprone molecule (*c*)

Table 1

*Solvent dielectric constants of*, *absolute energy* ($E$, Hartree), *solvation energy* ($E_{solv}$, kcal/mol), *dipole moment* (μ, Debye), *isotropic and anisotropic polarizabilities* (Bohr$^3$) *of the deferiprone molecule in solution phases*

| Phase | ε | $E_T$ | $E_{solv}$ | μ | $\alpha_{xx}$ | $\alpha_{yy}$ | $\alpha_{zz}$ | $\alpha_{iso}$ | $\alpha_{aniso}$ |
|---|---|---|---|---|---|---|---|---|---|
| Gas | — | –477.299 | — | 7.01 | 132.13 | 99.17 | 58.48 | 96.59 | 63.89 |
| Chloroform | 4.71 | –477.3105 | –7.18 | 9.16 | 164.96 | 120.89 | 69.86 | 118.57 | 82.44 |
| Chlorobenzene | 5.70 | –477.3113 | –7.70 | 9.32 | 167.33 | 122.52 | 70.99 | 120.28 | 83.50 |
| THF | 7.43 | –477.3123 | –8.31 | 9.51 | 170.09 | 124.45 | 72.39 | 122.31 | 84.67 |
| Methylenechloride | 8.93 | –477.3128 | –8.67 | 9.62 | 171.69 | 125.57 | 73.25 | 123.50 | 85.31 |
| Quinoline | 9.16 | –477.3129 | –8.71 | 9.64 | 171.90 | 125.71 | 73.36 | 123.66 | 85.39 |
| Isoquinoline | 11.00 | –477.3134 | –9.01 | 9.73 | 173.23 | 126.65 | 74.10 | 124.66 | 85.90 |

the total energy and the stabilization energy of solvents, respectively. From Table 1, we can see that the calculated energy is dependent on the size of the dielectric constant of solvents. The energies $E_T$ decrease in PCM with increasing dielectric constants of solvents. On the other hand, the $E_{solv}$ values indicate the increasing stability in more polar solvents. This is because a dipole in the molecule induces a dipole in the medium. Then, the electric field applied to the solute by the solvent dipole, in turn, interacts with the molecular dipole. These interactions lead to the net stabilization. This suggests that the deferiprone molecule is more stable in polar solvents rather than in the gas phase. There is a linear correlation between the dielectric constants and $E_{solv}$

$$E_{solv} = -0.289\varepsilon - 6.0037; \quad R^2 = 0.9566.$$

**Dipole moments.** Dipole moment values of deferiprone in the gas phase and different media are listed in Table 1. Fig. 1, *b* demonstrates the direction of a dipole moment in the molecule. These values show that the solvent effect on the stabilization energy is in parallel with that on the dipole moment of the solute. There is a linear relationship between the solvent stabilization energies and the dipole moments of deferiprone in the set of solvents (with the correlation coefficient of 1.00). Namely, at higher solvent polarity there is a larger dipole moment and a higher stabilization energy. Also, there is a linear correlation between the dipole moment and the dielectric constant

$$\mu = 0.1111\varepsilon + 9.1095; \quad R^2 = 0.9306.$$

**Polarizability.** Isotropic and anisotropic polarizability values for the deferiprone molecule in the gas phase and different media are listed in Table 1. The polarizability is the measure of a distortion of a molecule in the electric field. These values show that the solvent effect on the isotropic and anisotropic polarizabilities is in parallel with that on the dipole moment of the solute. There is a good linear relationship between the isotropic and anisotropic polarizabilities and the dipole moments of the complex in the set of solvents ($R^2$ = 1.00, and 0.9991, respectively). Namely, the larger the dipole moment of the solute is, the higher the isotropic and anisotropic polarizabilities at higher solvent polarity. Also, there is a good correlation between the isotropic and anisotropic polarizabilities and the dielectric constant with the correlation coefficients 0.9589 and 0.9449, respectively.

**Structural properties.** The deferiprone molecule contains one six-membered ring. The optimized structural parameters (bond lengths and bond angles) for the thermodynamically preferred geometry of deferiprone, determined at the M062X level using the 6-311++G(*d*,*p*) basis set, are reported in Table 2.

**CC *bond lengths.*** In the title molecule, the calculated C5C6 and C2C3 bond lengths are 1.361 and 1.360 Å in the gas phase, respectively. On the other hand, the calculated C1C2 and C6C1 bond lengths are 1.460 and 1.435 Å, respectively. The extension of these bond lengths rather than C5C6 and C2C3 bonds confirms the presence of a double bond character in C5C6 and C2C3 bonds. These bond lengths are compatible with the resonance forms of deferiprone (Fig. 1, *c*). These bond lengths increase with increasing dielectric constants of solvents. The C1C2 and C6C1 bond lengths decrease with increasing dielectric constants of solvents. The other bond lengths increase with increasing dielectric constants of solvents.

Table 2

*CC and CO bond lengths* (Å) *for the deferiprone molecule in the vacuum and solution phases and correlation coefficients of the solvent dielectric constant and experimental value*

| Phase | C1C2 | C1O1 | C2C3 | C2O2 | C3N4 | N4C5 | C5C6 | C6C1 | $R^2$ |
|---|---|---|---|---|---|---|---|---|---|
| Exp | 1.430 | 1.272 | 1.376 | 1.356 | 1.360 | 1.352 | 1.364 | 1.407 | — |
| Gas | 1.460 | 1.235 | 1.360 | 1.349 | 1.388 | 1.357 | 1.361 | 1.435 | 0.9523 |
| Chloroform | 1.452 | 1.247 | 1.363 | 1.354 | 1.382 | 1.353 | 1.365 | 1.429 | 0.9672 |
| Chlorobenzene | 1.451 | 1.248 | 1.363 | 1.354 | 1.382 | 1.353 | 1.365 | 1.428 | 0.9682 |
| THF | 1.450 | 1.249 | 1.364 | 1.355 | 1.381 | 1.353 | 1.365 | 1.428 | 0.9693 |
| Methylenechloride | 1.450 | 1.250 | 1.364 | 1.355 | 1.381 | 1.353 | 1.365 | 1.427 | 0.9700 |
| Quinoline | 1.450 | 1.250 | 1.364 | 1.355 | 1.381 | 1.353 | 1.365 | 1.427 | 0.9701 |
| Isoquinoline | 1.450 | 1.250 | 1.364 | 1.355 | 1.381 | 1.352 | 1.366 | 1.427 | 0.9706 |
| $R^2$ | 0.9575 | 0.9577 | 0.9548 | 0.9589 | 0.9568 | 0.9612 | 0.9581 | 0.9585 | — |

Table 3

*Frontier orbital energies* (a.u.), HOMO-LUMO *gap* (eV), *hardness* (eV), *softness* ($eV^{-1}$), *chemical potential* (eV), *electrophilicity* (eV), *wavelength* (nm), *oscillator strengths*, *and electric dipole moments* (a.u.) *for the most intense electronic transition in the deferiprone molecule in the vacuum and solution phases*

| Phase | HOMO | LUMO | $\Delta E$ | η | S | μ | ω | $\lambda_{max}$ | $f$ | μ |
|---|---|---|---|---|---|---|---|---|---|---|
| Gas | –0.2608 | –0.0175 | 6.62 | 3.31 | 0.30 | –3.79 | 1.44 | 176.52 | 0.41 | 2.38 |
| Chloroform | –0.2672 | –0.0059 | 7.11 | 3.55 | 0.28 | –3.72 | 1.29 | 179.75 | 0.55 | 3.27 |
| Chlorobenzene | –0.2677 | –0.0053 | 7.14 | 3.57 | 0.28 | –3.71 | 1.29 | 180.14 | 0.55 | 3.27 |
| THF | –0.2684 | –0.0046 | 7.18 | 3.59 | 0.28 | –3.71 | 1.28 | 179.66 | 0.56 | 3.29 |
| Methylenechloride | –0.2688 | –0.0043 | 7.20 | 3.60 | 0.28 | –3.71 | 1.28 | 179.79 | 0.56 | 3.32 |
| Quinoline | –0.2688 | –0.0042 | 7.20 | 3.60 | 0.28 | –3.72 | 1.28 | 176.95 | 0.48 | 2.80 |
| Isoquinoline | –0.2692 | –0.0040 | 7.22 | 3.61 | 0.28 | –3.72 | 1.28 | 176.97 | 0.48 | 2.82 |

**CO *bond lengths.*** The shorting of the C1O1 bond length rather than the C2O2 bond is compatible with the existence of a double bond character in the C1O1 bond. These bonds are shorter in the solution phase than those in the gas phase.

The relations between the experimental [ 19 ] and calculated bond distances are examined in the gas and solution phases and correlation coefficients are reported in Table 2. These values indicate a good correlation between the predicted and observed bond distances.

**CN *bond lengths.*** The C3N4 and N4C5 bond lengths are 1.388 and 1.357 Å, respectively. These bonds are shorter in the solution phase than those in the gas phase. The bond lengths decrease with increasing dielectric constants of solvents.

**Frontier orbital energies.** The influence of the solvent nature is reflected not only in the geometric parameters of the molecules, but also in the energies of frontier orbitals. It is well-known that the frontier orbital energy and HOMO-LUMO gap values are closely related to the optical and electronic properties.

The inclusion of solvation effects also leads to changes in the molecular orbital energies (Table 3). In a solution, HOMO is stabilized, with respect to the corresponding values in vacuum, but LUMO is destabilized. A good linear relation is seen between the frontier orbital energies and the dielectric constants

$$E(\text{HOMO}) = -0.0003\varepsilon - 0.2659; \quad R^2 = 0.9596;$$
$$E(\text{LUMO}) = 0.0003\varepsilon - 0.0071; \quad R^2 = 0.9396.$$

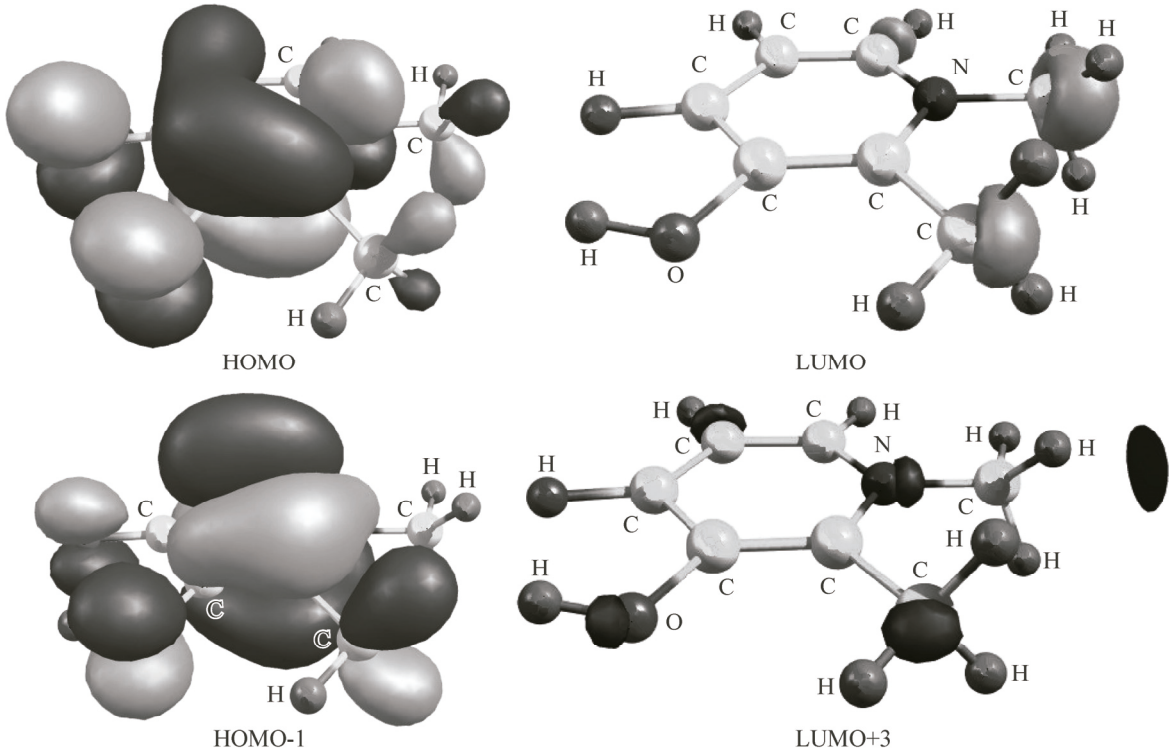


*Fig. 2.* Plots of HOMO, LUMO, HOMO-1, and LUMO+3 in the deferiprone molecule

The HOMO-LUMO gaps in solvated media are higher than the corresponding computed values in vacuum. A good linear relation is seen between the HOMO-LUMO gaps and the dielectric constants

$$\Delta E(\text{HOMO-LUMO}) = 0.0169\ \varepsilon + 7.0411; \quad R^2 = 0.9501.$$

To get insight into the effect on the optical and electronic properties, the distributions of the frontier orbitals for these molecules are investigated, and their sketches are plotted in Fig. 2. The molecular orbital analysis shows that HOMO has the π character, as visualized in Fig. 2 for deferiprone.

Table 3 reveals that the chemical potentials of the solution phases are less than that of the gas phase. The study of the solvent effect on the chemical potential values also shows a decrease in these values with an increase in the dielectric constants

$$\mu = -0.003\varepsilon + 1.3064; \quad R^2 = 0.9272.$$

The electrophilicity values of the deferiprone molecule in the vacuum and solution phases are gathered in Table 3. From these calculations, it follows that the electrophilicity increases in the solution phase vs. the vacuum phase. On the other hand, these values increase with increasing dielectric constants. There is a good correlation between the chemical potential and electrophilicity values and the dielectric constants

$$\omega = 0.0169\varepsilon + 7.0411; \quad R^2 = 0.9501.$$

**Local reactivity descriptors.** Based on Mulliken atomic charges, nucleophilic reactivity descriptors ($f_k^-, s_k^-, \omega_k^-$) for deferiprone are gathered in Table 4. The maximum values of the local nucleophilic reactivity descriptors ($f_k^-, s_k^-, \omega_k^-$) at N4 indicate that these sites are susceptible to electrophilic attack.

Using Mulliken atomic charges, the electrophilic reactivity descriptors ($f_k^+, s_k^+, \omega_k^+$) [20], are listed in Table 4. The maximum values of the local electrophilic reactivity descriptors ($f_k^+, s_k^+, \omega_k^+$) of deferiprone at the C3′ atom signify that this site is more disposed to nucleophilic attack.

Table 4

*Nucleophilic reactivity descriptors* ($f_k^-, s_k^-, \omega_k^-$), *electrophilic reactivity descriptors* ($f_k^-, s_k^-, \omega_k^-$) *for the deferiprone molecule*

| Parameter | $f^+$ | $f^-$ | $f^0$ | $S^+$ | $S^-$ | $s^0$ | $\omega^+$ | $\omega^-$ | $\omega^0$ |
|---|---|---|---|---|---|---|---|---|---|
| C1 | 0.3910 | –0.8254 | –0.2172 | 0.1181 | –0.2493 | –0.0656 | 0.5646 | –1.1918 | –0.3136 |
| O1 | 0.7633 | –0.6146 | 0.0743 | 0.2305 | –0.1856 | 0.0225 | 1.1021 | –0.8875 | 0.1073 |
| C2 | 0.3569 | 0.0329 | 0.1949 | 0.1078 | 0.0099 | 0.0589 | 0.5153 | 0.0475 | 0.2814 |
| O2 | 0.4332 | –0.2745 | 0.0793 | 0.1308 | –0.0829 | 0.0240 | 0.6255 | –0.3964 | 0.1145 |
| C3 | –0.1886 | 0.0469 | –0.0708 | –0.0570 | 0.0142 | –0.0214 | –0.2723 | 0.0678 | –0.1022 |
| C3′ | 0.7801 | –0.7702 | 0.0049 | 0.2356 | –0.2326 | 0.0015 | 1.1263 | –1.1121 | 0.0071 |
| N4 | –0.0628 | 0.2392 | 0.0882 | –0.0190 | 0.0723 | 0.0266 | –0.0907 | 0.3455 | 0.1274 |
| C4′ | 0.3106 | –0.3444 | –0.0169 | 0.0938 | –0.1040 | –0.0051 | 0.4484 | –0.4972 | –0.0244 |
| C5 | –0.0980 | –0.5265 | –0.3123 | –0.0296 | –0.1590 | –0.0943 | –0.1415 | –0.7602 | –0.4509 |
| C6 | 0.1526 | 0.2030 | 0.1778 | 0.0461 | 0.0613 | 0.0537 | 0.2203 | 0.2932 | 0.2567 |

Table 5

*Thermodynamic parameters for the deferiprone molecule at various temperatures in the gas phase*

| $T$ | $G$ | $H$ | $S$ | $C_v$ | $T$ | $G$ | $H$ | $S$ | $C_v$ |
|---|---|---|---|---|---|---|---|---|---|
| 100 | –477.152646 | –477.142098 | 66.188 | 14.273 | 600 | –477.231726 | –477.108882 | 128.476 | 61.161 |
| 200 | –477.164395 | –477.138626 | 80.851 | 25.258 | 700 | –477.253021 | –477.098331 | 138.670 | 67.098 |
| 300 | –477.178332 | –477.133447 | 93.886 | 35.687 | 800 | –477.275889 | –477.086915 | 148.229 | 72.057 |
| 400 | –477.194275 | –477.126653 | 106.085 | 45.452 | 900 | –477.300233 | –477.074773 | 157.198 | 76.241 |
| 500 | –477.212109 | –477.118393 | 117.615 | 54.002 | 1000 | –477.325963 | –477.062015 | 165.630 | 79.801 |

**Thermodynamic parameters.** The thermochemical analysis was carried out for deferiprone. According to the statistical thermodynamic principle, heat capacities ($C_v$, cal·K$^{-1}$·mol$^{-1}$), entropies ($S$, cal·K$^{-1}$·mol$^{-1}$), free energies ($G$, a.u.) and enthalpies ($H$, a.u.) in the range 100—10000 K were obtained and are gathered in Table 5. As it is obvious from Table 5, the $C_v$, $S$, and $H$ thermodynamic functions of deferiprone increase with an increase in the temperature. The reason is that the vibrational motion is invigorated at higher temperatures and makes more contributions to the thermodynamic functions, although the main contributions are due to the translation and rotation of the molecules at lower temperatures. The relationships between the temperature range 100—1000 K and the thermodynamic functions are expressed as

$$G = -9\cdot10^{-8}T^2 - 1\cdot10^{-4}T - 477.14, \quad R^2 = 1;$$
$$H = 6\cdot10^{-8}T^2 + 3\cdot10^{-5}T - 477.15, \quad R^2 = 0.9996;$$
$$S = -4\cdot10^{-5}T^2 + 0.1487T + 52.147, \quad R^2 = 0.9999;$$
$$C_v = -5\cdot10^{-5}T^2 + 0.1305T + 1.5333, \quad R^2 = 0.9999.$$

**Electronic spectra.** We investigated the most intense electronic transition ($\lambda_{max}$) of the molecule. The wavelength, oscillator strength, electric dipole moments, and the transition composition btained by TD-DFT calculations are given in Table 3. Theoretical calculations of the deferiprone molecule reveal that the HOMO-1 → LUMO+3 transition is the major contribution to this electronic transition.

The addition of solvation effects directly caused changes in $\lambda_{max}$ (Table 3). In the solution, the $\lambda_{max}$ is red-shifted as compared to the corresponding values in the vacuum.

**Hyperpolarizability.** The hyperpolarizability (β) reported here is defined as

$$\beta_{tot} = (\beta_x^2 + \beta_y^2 + \beta_z^2)^{1/2},$$

Table 6

*Hyperpolarizability values for the deferiprone molecule in the vacuum and solution phases. Unit of* $\beta_{tot}$ *is esu. Other parameters are in* a.u. (1 a.u. = $8.63922 \cdot 10^{-33}$ esu)

| Parameter | Gas | Chloroform | Chlorobenzene | THF | Methylenechloride | Quinoline | Isoquinoline |
|---|---|---|---|---|---|---|---|
| $\beta_{XXX}$ | 255.17 | 441.65 | 459.34 | 481.10 | 494.08 | 495.74 | 506.85 |
| $\beta_{XXY}$ | –21.62 | –57.40 | –61.39 | –66.49 | –69.56 | –69.96 | –72.65 |
| $\beta_{XYY}$ | –89.03 | –189.77 | –199.11 | –210.41 | –217.20 | –218.07 | –223.83 |
| $\beta_{YYY}$ | –196.58 | –326.27 | –337.38 | –350.74 | –358.66 | –359.67 | –366.37 |
| $\beta_{XXZ}$ | 11.76 | 10.08 | 10.00 | 9.83 | 9.82 | 9.81 | 9.72 |
| $\beta_{XYZ}$ | –1.83 | –1.83 | –1.85 | –1.85 | –1.86 | –1.86 | –1.91 |
| $\beta_{YYZ}$ | –4.78 | –4.93 | –4.95 | –4.97 | –4.97 | –4.97 | –4.97 |
| $\beta_{XZZ}$ | 63.57 | 76.84 | 77.92 | 79.23 | 79.99 | 80.10 | 80.78 |
| $\beta_{YZZ}$ | –26.31 | –39.92 | –41.48 | –43.47 | –44.70 | –44.86 | –45.94 |
| $\beta_{ZZZ}$ | 8.54 | 5.97 | 5.91 | 5.84 | 5.80 | 5.80 | 5.71 |
| $\beta_{tot}$ | $2.9\times10^{-30}$ | $4.63\times10^{-30}$ | $4.78\times10^{-30}$ | $5.00\times10^{-30}$ | $5.12\times10^{-30}$ | $5.13\times10^{-30}$ | $5.24\times10^{-30}$ |
| $\beta_{tot}\times10^{30}$ | 2.90 | 4.63 | 4.80 | 5.00 | 5.12 | 5.13 | 5.24 |
| $\beta_X$ | $1.98\times10^{-30}$ | $2.84\times10^{-30}$ | $2.92\times10^{-30}$ | $3.02\times10^{-30}$ | $3.08\times10^{-30}$ | $3.09\times10^{-30}$ | $3.14\times10^{-30}$ |
| $\beta_Y$ | $-2.1\times10^{-30}$ | $-3.66\times10^{-30}$ | $-3.80\times10^{-30}$ | $-3.98\times10^{-30}$ | $-4.08\times10^{-30}$ | $-5.00\times10^{-30}$ | $-4.19\times10^{-30}$ |
| $\beta z$ | $1.34\times10^{-31}$ | $9.61\times10^{-32}$ | $9.465\times10^{-32}$ | $9.25\times10^{-32}$ | $9.20\times10^{-32}$ | $9.18\times10^{-32}$ | $9.04\times10^{-32}$ |

where

$$\beta_i = \frac{1}{3} \sum_{k=x,y,z} (\beta_{ikk'} + \beta_{kik} + \beta_{kki}); \qquad i = x, y, z.$$

A theoretical investigation plays a fundamental role in the comprehension of structure-property correlations. Theoretical investigations assist in designing novel NLO chromophores. The first electrostatic hyperpolarizability ($\beta_{tot}$) of deferiprone has been calculated in both gas phase and various solvents. According to Table 6 values, the largest $\beta_{tot}$ values are found at higher polarities. Also, the $\beta_{tot}$ values increase from the vacuum phase to different solvents. The first hyperpolarizability of the title compound depends on the dielectric constant of the media and the Onsager function [ 21 ] that is specific for a dipolar reaction field interaction in the solvation process [ 22 ]. The corresponding equations are

$$10^{30}\,\beta_{tot} = 0.0963\varepsilon + 4.2334, \quad R^2 = 0.9625;$$

$$10^{30}\,\beta_{tot} = 7.6897\,\frac{(\varepsilon - 1)}{(2\varepsilon + 1)} + 1.8877, \quad R^2 = 0.9994.$$

**$^{1}$H and $^{13}$C NMR chemical shifts.** The theoretical and experimental $^{1}$H and $^{13}$C NMR chemical shifts of the deferiprone molecule are listed in Table 7. Relative chemical shifts were calculated using the corresponding TMS shielding estimated in advance at the same theoretical level as the reference. The GIAO method has been used for NMR calculations.

**$^{1}$H NMR.** The trend of proton signals in deferiprone is: H6 > H5 > H(Me4) > H(Me3). Based on this trend, it is found that the H6, and H5 chemical shifts are higher than those of hydrogen atoms of methyl groups. Consequently, the electronic charge densities around H5 and H6 are lower than those around other hydrogen atoms. The chemical shift values increase in the solution phase vs. the vacuum phase. On the other hand, these chemical shift values increase with increasing dielectric constants of solvents.

**$^{13}$C NMR.** The signal of the carbonyl carbon atom (C1) in the gas phase was detected at 184.2 ppm. This atom has a larger chemical shift than those of the other carbon atoms in the molecule owing to the oxygen atom electronegativity. The study of the solvent effect on the $^{13}$C NMR chemical

Table 7

$^{1}$H *and* $^{13}$C NMR *chemical shifts for the deferiprone molecule* (*in* ppm) *in the vacuum and solution phases and correlation coefficients of the solvent dielectric constant and experimental value*

$^{1}$H NMR

| Phase | H5 | H6 | Me4 | Me3 | $R^2$ | Molecule | H5 | H6 | Me4 | Me3 | $R^2$ |
|---|---|---|---|---|---|---|---|---|---|---|---|
| Exp* | 7.07 | 8.15 | 3.95 | 2.47 | — | Methylenechloride | 6.58 | 7.61 | 3.53 | 1.94 | 1.00 |
| Gas | 6.26 | 6.99 | 3.19 | 1.51 | 1.00 | Quinoline | 6.58 | 7.62 | 3.53 | 1.94 | 1.00 |
| Chloroform | 6.56 | 7.54 | 3.50 | 1.90 | 1.00 | Isoquinoline | 6.58 | 7.63 | 3.53 | 1.95 | 1.00 |
| Chlorobenzene | 6.57 | 7.56 | 3.51 | 1.91 | 1.00 | $R^2$ | 0.9506 | 0.9573 | 0.9574 | 0.9588 | — |
| THF | 6.57 | 7.59 | 3.52 | 1.93 | 1.00 | | | | | | |

$^{13}$C NMR

| Phase | C6 | C5 | C3 | C2 | C1 | Me4 | Me3 | $R^2$ |
|---|---|---|---|---|---|---|---|---|
| Exp | 110.3 | 138.5 | 140.7 | 143.0 | 159.7 | 43.6 | 12.5 | — |
| Gas | 123.7 | 150.5 | 136.6 | 160.5 | 184.2 | 38.7 | 8.1 | 0.9837 |
| Chloroform | 123.7 | 153.4 | 142.2 | 159.8 | 185.9 | 40.2 | 8.8 | 0.9896 |
| Chlorobenzene | 123.7 | 153.6 | 142.6 | 159.7 | 186.0 | 40.3 | 8.8 | 0.9899 |
| THF | 123.7 | 153.9 | 143.1 | 159.6 | 186.1 | 40.5 | 8.9 | 0.9904 |
| Methylenechloride | 123.7 | 154.0 | 143.3 | 159.6 | 186.2 | 40.6 | 8.9 | 0.9906 |
| Quinoline | 123.7 | 154.1 | 143.4 | 159.6 | 186.2 | 40.6 | 8.9 | 0.9907 |
| Isoquinoline | 123.7 | 154.2 | 143.6 | 159.5 | 186.2 | 40.7 | 9.0 | 0.9909 |
| $R^2$ | 0.9653 | 0.9586 | 0.9568 | 0.9606 | 0.9384 | 0.9595 | 0.9582 | — |

* *Šebestik J.*, *Šafařík M.*, *Bouř P.* // Inorg. Chem. – 2012. – **51**. – P. 4473 – 4481.

shift exhibits that the C6 and C2 chemical shifts decrease in the solution phase vs. the vacuum phase. For other carbon atoms, these values increase in the solution phase.

The relations between the experimental and calculated chemical shifts are examined in the gas and solution phases and correlation coefficients are reported in Table 7. These values indicate a good correlation between the predicted and observed proton and carbon chemical shifts.

**Vibrational analysis.** The deferiprone molecule possesses the C1 point group symmetry. This compound consists of 19 atoms which construct 51 normal modes of fundamental vibrations. Vibrational spectral assignments of the title compound were performed by the *ab initio* M062X method using the 6-311++G(*d*,*p*) basis set. These calculations show that.

**$CH_3$.** The stretching vibrations of $CH_3$ are expected in the range 2900—3050 $cm^{-1}$ [ 23 ]. The band at 3070.26 $cm^{-1}$ results from the symmetric stretching $\upsilon_s(CH_3)$ in which all three of the C—H bonds expand and contract in-phase. The experimental data on this stretching is 2940 $cm^{-1}$ [ 19 ].

**C=O.** The band at 1706.83 $cm^{-1}$ is attributed to the C1=O1 bond stretching. The experimental data on this stretching is 1630 $cm^{-1}$.

**O—H.** The bands at 1309.29 and 1395.57 $cm^{-1}$ are attributed to the O—H bond bending. The band at 3675.28 $cm^{-1}$ corresponds to the O—H bond stretching. The experimental data on this stretching is 3150 $cm^{-1}$.

**CH.** The band at 3236.54 $cm^{-1}$ corresponds to the symmetric stretching of CH bonds of C(5)H(5) and C(6)H(6), all together. The band at 3217.62 $cm^{-1}$ describes the asymmetric stretching of CH bonds of C(5)H(5) and C(6)H(6).

**CN.** The band at 1057.12 $cm^{-1}$ is attributed to the C—N bond stretching. The experimental data on this stretching is 1250 $cm^{-1}$.

**C=C.** The bands at 1736.07 and 1636.04 $cm^{-1}$ are due to the symmetric and asymmetric stretching of C2=C3 and C5=C6 bonds, respectively. Concurrently, two C=C bonds expand or contract in

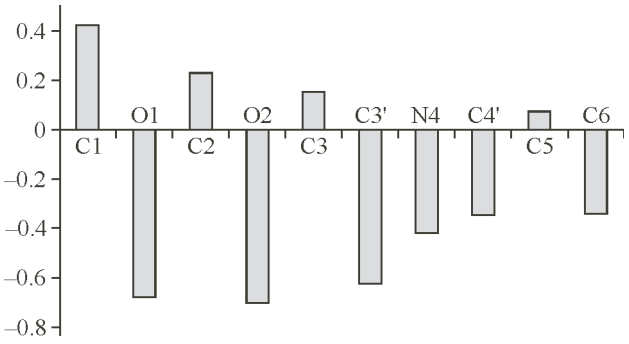


*Fig. 3.* Distributions of NBO charges in the deferiprone molecule

symmetric stretching. However, at the same time, these C=C bonds expand and contract in asymmetric stretching.

The relations between the experimental and calculated wavenumbers are examined in gas for the stretching of OH, CO, CH, and CN bonds. These values indicate a good correlation between the predicted and observed wavenumbers

$$\bar{\nu}(\text{theo}) = 1.266\ \bar{\nu}(\text{exp}) - 462.96; \qquad R^2 = 0.9832.$$

**NBO analysis.** The NBO analysis is a helpful method for the investigation of attractive features of a molecular structure.

The NBO analysis of the atomic charges was carried out to obtain the charge distribution (Fig. 3). The magnitudes of the carbon atomic charges of the compounds were found to be both positive and negative. The maximum atomic charge was obtained for C1 due to the effect of the negatively charged oxygen atom. Moreover, based on this method, the O2 atom is considered as a more basic site.

The NBO theory lets the determination of the hybridization of atomic lone pairs and atoms included in bond orbitals. The calculated natural orbital occupancy (″natural population″ of the orbital, or number of electrons) and the hybridization of C—C, C—N and C—O bonds of the title molecule are listed in Table 8.

Table 9 reports the strongest second order interaction energies $E^{(2)}$ between the donor and acceptor orbitals in deferiprone. The second order Fock matrix has been used to estimate the donor-acceptor

Table 8

*Natural orbital occupancies* (NBOs) *and hybrids of* C—C, C—N *and* C—O *bonds in the deferiprone molecule*

| Bond | Occupancy | $ED_A$, % | $ED_B$, % | NBO |
|---|---|---|---|---|
| σ(C1—C2) | 1.97383 | 48.07 | 51.93 | $0.6933(sp^{2.15})_{C1} + 0.7206(sp^{1.91})_{C2}$ |
| σ(C1—C6) | 1.97754 | 49.38 | 50.62 | $0.7027(sp^{1.73})_{C1} + 0.7115(sp^{1.97})_{C6}$ |
| σ(C1—O1) | 1.99423 | 36.12 | 63.88 | $0.6010(sp^{2.19})_{C1} + 0.7992(sp^{1.46})_{O1}$ |
| π(C1—O1) | 1.98082 | 28.45 | 71.55 | $0.5333(p^{1.00})_{C1} + 0.8459(p^{1.00})_{O1}$ |
| σ(C2—C3) | 1.97365 | 49.45 | 50.55 | $0.7032(sp^{1.51})_{C2} + 0.7110(sp^{1.61})_{C3}$ |
| π(C2—C3) | 1.79616 | 48.97 | 51.03 | $0.6998(p^{1.00})_{C2} + 0.7144(p^{1.00})_{C3}$ |
| σ(C2—O2) | 1.99218 | 34.03 | 65.97 | $0.5834(sp^{2.89})_{C2} + 0.8122(sp^{1.96})_{O2}$ |
| σ(C3—N4) | 1.98045 | 36.54 | 63.46 | $0.6044(sp^{2.64})_{C3} + 0.7966(sp^{1.90})_{N4}$ |
| σ(C3—C3′) | 1.98044 | 51.49 | 48.51 | $0.7176(sp^{1.92})_{C3} + 0.6965(sp^{2.52})_{C3'}$ |
| σ(N4—C5) | 1.98361 | 63.87 | 36.13 | $0.7992(sp^{1.840})_{N4} + 0.6011(sp^{2.47})_{C5}$ |
| σ(N4—C4′) | 1.98802 | 64.10 | 35.90 | $0.8006(sp^{2.30})_{N4} + 0.5992(sp^{3.21})_{C4'}$ |
| σ(C5—C6) | 1.97789 | 50.81 | 49.19 | $0.7128(sp^{1.44})_{C5} + 0.7014(sp^{1.77})_{C6}$ |
| π(C5—C6) | 1.82033 | 45.64 | 54.36 | $0.6756(p^{1.00})_{C5} + 0.7373(p^{1.00})_{C6}$ |

Table 9

*Second order perturbation theory analysis of the Fock matrix in the* NBO *basis corresponding to the intramolecular bonds of the deferiprone molecule*

| Donor NBO ($i$) → Acceptor NBO ($j$) | $E^{(2)}$, kcal/mol | $E(j) - E(i)$, a.u. | $F(i,j)$, a.u. |
|---|---|---|---|
| π(C2—C3) → π*(C1—O1) | 25.58 | 0.40 | 0.094 |
| π(C5—C6) → π*(C1—O1) | 30.51 | 0.39 | 0.103 |
| LP(1) (N4) → π*(C2—C3) | 41.91 | 0.39 | 0.119 |
| LP(1) (N4) → π*(C5—C6) | 55.95 | 0.38 | 0.135 |
| LP(2) (O2) → π*(C2—C3) | 37.55 | 0.45 | 0.121 |
| LP(1) (O1) → RY*(1) (C1) | 14.83 | 1.89 | 0.150 |
| LP(2) (O1) → σ*(C1—C2) | 21.11 | 0.85 | 0.121 |
| LP(2) (O1) → σ*(C1—C6) | 20.39 | 0.89 | 0.122 |

interactions in the NBO analysis [ 24 ]. For each donor ($i$) and acceptor ($j$), the stabilization energy $E^{(2)}$ related to the delocalization $i \rightarrow j$ is evaluated as

$$E^{(2)} = -q_i \frac{(F_{i,j})^2}{\varepsilon_j - \varepsilon_i}.$$

The larger $E^{(2)}$ value denotes a significant interaction between electron donors and acceptors. The title molecule exhibits the maximum stabilization energy of 55.95 kJ/mol through the interaction between LP(1) of N4 and π*(C5—C6). It could be revealed that the anti-bonding C5—C6 NBO has 49.19 % of the C5 character in $sp^{1.44}$ hybrid and 50.81 % of the C6 character in the $sp^{1.77}$ hybrid. The $sp^{1.44}$ hybrid on C5 has 59.05 % $p$ characters, and the $sp^{2.90}$ hybrid on C6 has a 63.90 % $p$-character. The coefficients of 0.7014 and –0.7128 are found to be the identified polarization coefficients of C5 and C6. The extents of these coefficients illustrate the significance of the two hybrids in the bond formation. Another important interaction in title molecule includes the interactions of LP(1) of N4 with π*(C2—C3) and has stabilization energies of 41.91 kcal/mol.

## CONCLUSIONS

In this paper, the structural and spectroscopic properties of deferiprone were studied at the M062X/6-311++G($d$,$p$) level of theory, which indicated:

1. Solvation energy values indicate the increase in the stability of the title molecule in more polar solvents.
2. The geometry, dipole moments, polarizability of the molecule are affected by the solvent. With an increase in the polarity of solvents, the dipole moment increased.
3. The analysis of the electronic spectra shows that the highest transition intensity is assigned to the HOMO-1 → LUMO+3 LUMO transition.
4. The experimental values of the vibrational frequencies and chemical shifts indicate a good correlation with the calculated results.
5. The hyperpolarizability values increase from vacuum to the solution phase, and are dependent on the dielectric constants of the media and the Onsager function.
6. NBO analysis shows the maximum stabilization energy for the interaction between LP(1) of N4 and π*(C5—C6).

## *REFERENCES*

1. (a) *Sattarahmady N., Heli H., Moosavi-Movahedi A., Karimian K.* // Mol. Biol. Rep. – 2014. – **41**. – P. 1723. (b) *Olivieri N.F., Brittenham G.M., McLaren C.E., Templeton D.M., Cameron R.G., McClelland R.A., Burt A.D., Fleming K.A.* // New Eng. J. Med. – 1998. – **339**. – P. 417. (c) *Fosburg M.T., Nathan D.G.* // Blood. – 1990. – **76**. – P. 435. (d) *Olivieri N.F., Brittenham G.M., Matsui D., Berkovitch M., Blendis L.M.,*

*Cameron R.G., McClelland R.A., Liu P.P., Templeton D.M., Koren G.* // New Eng. J. Med. – 1995. – **332**. – P. 918.
2. (a) *Dorraji M.S., Azar V.P., Rasoulifard M.* // Eur. J. Pharm. Sci. – 2014. – **64**. – P. 9. (b) *Song D., Zhao L., Li Y., Hadziahmetovic M., Song Y., Dunaief J.L.* // Invest. Ophthalmol. Visual Sci. – 2014. – **55**. – P. 415. (c) *Song D., Zhao L., Li Y., Hadziahmetovic M., Song Y., Connelly J., Spino M., Dunaief J.L.* // Invest. Ophthalmol. Visual Sci. – 2014. – **55**. – P. 4525.
3. (a) *Harmatz P., Butensky E., Quirolo K., Williams R., Ferrell L., Moyer T., Golden D., Neumayr L., Vichinsky E.* // Blood. – 2000. – **96**. – P. 76. (b) *Engle M.A., Erlandson M., Smith C.H.* // Circulation. – 1964. – **30**. – P. 698. (c) *Cohen A.* // Hematol. Oncol. Clin. N. Am. – 1987. – **1**. – P. 521.
4. (a) *Modell B., Khan M., Darlison M.* // The Lancet. – 2000. – **355**. – P. 2051. (b) *Borgna-Pignatti C., Rugolotto S., De Stefano P., Zhao H., Cappellini M.D., Del Vecchio G.C., Romeo M.A., Forni G.L., Gamberini M.R., Ghilardi R.* // Haematologica. – 2004. – **89**. – P. 1187.
5. (a) *Kontoghiorghes G.J.* // Hemoglobin. – 2006. – **30**. – P. 183. (b) *Richardson D.R.* // The Lancet. – 2002. – **360**. – P. 501. (c) *Kontoghiorghes G.J., Efstathiou A., Ioannou-Loucaides S., Kolnagou A.* // Hemoglobin. – 2008. – **32**. – P. 217. (d) *Yasumoto E., Nakano K., Nakayachi T., Morshed S.R.M., Hashimoto K., Kikuchi H., Nishikawa H., Kawase M., Sakagami H.* // Anticancer Res. – 2004. – **24**. – P. 755.
6. *Chenoufi N., Drénou B., Loréal O., Pigeon C., Brissot P., Lescoat G.* // Biochem. Pharmacol. – 1998. – **56**. – P. 431.
7. (a) *Yadegari H., Jabbari A., Heli H., Moosavi-Movahedi A., Majdi S.* // J. Braz. Chem. Soc. – 2008. – **19**. – P. 1017. (b) *Georgiou N.A., van der Bruggen T., Oudshoorn M., Nottet H.S., Marx J.J., van Asbeck B.S.* // J. Infect. Dis. – 2000. – **181**. – P. 484.
8. *Sappey C., Boelaert J.R., Legrand-Poels S., Forceille C., Favier A., Piette J.* // AIDS Res. Hum. Retroviruses. – 1995. – **11**. – P. 1049.
9. *Ganeshaguru K., Hoffbrand A.V., Grady R.W., Cerami A.* // Biochem. Pharmacol. – 1980. – **29**. – P. 1275.
10. *Tomasi J., Mennucci B., Cammi R.* // Chem. Rev. – 2005. – **105**. – P. 2999.
11. *Frisch M.J., Trucks G.W., Schlegel H.B., Scuseria G.E., Robb M.A., Cheeseman J.R., Scalman G., Barone V., Mennucci B., Petersson G.A., Nakatsuji H., Caricato M., Li X., Hratchian H.P., Izmaylov A.F., Bloino J., Zheng G., Sonnenberg J.L., Hada M., Ehara M., Toyota K., Fukuda R., Hasegawa J., Ishida M., Nakajima T., Honda Y., Kitao O., Nakai H., Vreven T., Montgomery J.A. Jr., Peralta J.E., Ogliaro F., Bearpark M., Heyd J.J., Brothers E., Kudin K.N., Staroverov V.N., Kobayashi R., Normand J., Raghavachari K., Rendell A., Burant J.C., Iyengar S.S., Tomasi J., Cossi M., Rega N., Millam J.M., Klene M., Knox J.E., Cross J.B., Bakken V., Adamo C., Jaramillo J., Gomperts R., Stratmann R.E., Yazyev O., Austin A.J., Cammi R., Pomelli C., Ochterski J.W., Martin R.L., Morokuma K., Zakrzewski V.G., Voth G.A., Salvador P., Dannenberg J.J., Dapprich S., Daniels A.D., Farkas O., Foresman J.B., Ortiz J.V., Cioslowski J., Fox D.J.* Gaussian 09. Revision A.02. – Wallingford, CT: Gaussian Inc., 2009.
12. *Krishnan R., Binkley J.S., Seeger R., Pople A.* // J. Chem. Phys. – 1980. – **72**. – P. 650.
13. *Zhao Y., Truhla D.G.* // J. Phys. Chem. – 2006. – **110**. – P. 5121.
14. *Reed A.E., Curtiss L.A., Weinhold F.* // Chem. Rev. – 1988. – **88**. – P. 899.
15. *Glendening E.D., Reed A.E., Carpenter J.E., Weinhold F.* NBO, version 3.1.
16. *Jamroz M.H.* Vibrational energy distribution analysis: VEDA 4 program – Warsaw, 2004.
17. *Wolinski K., Hinton J.F., Pulay P.* // J. Am. Chem. Soc. – 1990. – **112**. – P. 8251.
18. *Runge E., Gross E.K.U.* // Phys. Rev. Lett. – 1984. – **52**. – P. 997.
19. *Nelson W., Kappishins I., Rettig E., Rvig C.* // Can. J. Chem. – 1988. – **66**. – P. 123.
20. *Yang W., Mortier W.J.* // J. Am. Chem. Soc. – 1986. – **108**. – P. 5708.
21. *Onsager L.* // J. Am. Chem. Soc. – 1936. – **58**. – P. 1486.
22. (a) *Ray P.C., Leszczynski J.* // Chem. Phys. Lett. – 2004. – **339**. – P. 162. (b) *Clays K., Persoons A.* // Phys. Rev. Lett. – 1991. – **66**. – P. 2980. (c) *Lee H., An S.-Y., Cho M.* // J. Phys. Chem. B. – 1999. – **103**. – P. 4992.
23. (a) *Roeges N.P.G.* A Guide to Complete Interpretation of IR Spectra of Organic Structures. – New York: Wiley, 1994. (b) *Colthup N.B., Daly L.H., Wiberly S.E.* Introduction to Infrared and Raman Spectroscopy. – New York: Academic Press, 1975.
24. *Yang Y., Zhang W.J., Gao X.M.* // Int. J. Quantum Chem. – 2006. – **106**. – P. 1199.